EUCALL

The European Cluster of Advanced Laser Light Sources

Grant Agreement Number: 654220

Work Package 7 – PUCCA

Deliverable D7.2

Liquid Jet Capabilities

Lead Beneficiary: European XFEL

Authors: S. Schulz (European XFEL), M. Přeček (ELI Beamlines), J. Andreasson (ELI Beamlines), P. Brůža (ELI Beamlines), O. Kulyk (ELI Beamlines), A. Galler (European XFEL), S. Klumpp (DESY), C. Bressler (European XFEL)

Due date: 31 December 2016
Date of delivery: 31 December 2016

Project webpage: www.eucall.eu

Deliverable Type	
R = Report DEM = Demonstrator, pilot, prototype, plan designs DEC = Websites, patents filing, press & media actions, videos, etc. OTHER = Software, technical diagram, etc.	R
Dissemination Level	
PU = Public, fully open, e.g. web CO = Confidential, restricted under conditions set out in Model Grant Agreement CI = Classified, information as referred to in Commission Decision 2001/844/EC	PU

This project has received funding from the *European Union's Horizon 2020 research and innovation programme* under grant agreement No 654220

Table of Contents

This project has received funding from the *European Union's Horizon 2020 research and innovation programme* under grant agreement No 654220

A Abstract

Modern user facilities for X-ray generation, like the European XFEL and ELI, will deliver X-ray pulses with Ångström-wavelength and durations of single to tens of femtoseconds. To reveal dynamics at the molecular and atomic level, experiments will routinely be carried out in a pump-probe geometry where an external, optical laser pulse excites a specimen, while the ultrashort X-ray pulses are used to follow the development of the excitation. For this, the precise knowledge of the relative arrival time between the optical and the X-ray pulses is essential, and hence needs to be measured with a temporal precision of the order of the pulse duration. Moreover, this measurement has to be done ideally without deteriorating the pulses of the actual experiment and hence a key component is the interaction medium for this measurement. Established techniques are based on probing thin solid samples or foils with an optical laser pulse. Here an X-ray induced change of the electronic properties, e.g. refractive index, is exploited to retrieve the relative arrival time. With European XFEL and ELI Beamlines, two high repetition rate (up to 4.5 MHz) X-ray sources will soon become available, which set two significant challenges for arrival time measurements: First, the decay time of the material's modified property may be too large, as electronic processes can last for tens of nanoseconds, such that for a subsequent X-ray/optical pulse pair an already excited sample is probed, which alters the outcome of the timing retrieval. Secondly, the induced heat load into the sample from high repetition rate X-ray free-electron laser pulses can deteriorate or destroy the sample. Therefore, the capabilities of liquid jets are being investigated in this report, as these jets can be made fast flowing for shot-to-shot sample replacement while providing a thin, flat interaction region for high time resolution. Additionally, by choosing an appropriate solvent and solute, the effect exploited for the timing measurement can be tailored to some extent.

This project has received funding from the *European Union's Horizon 2020 research and innovation programme* under grant agreement No 654220

1 Introduction

In the following, the two facilities benefiting most from the investigation of the flat-sheet liquid jet capabilities and the timing tool developments are briefly introduced. Some of the methods for the high-repetition timing tools to be developed can be also potentially beneficial for the operation with other high-repetition sources, e.g. synchrotron slicing beamlines. Additional information on conceptual or technical details can be found in the references given below.

1.1 European XFEL

The European X-ray Free-Electron Laser (European XFEL, or sometimes just XFEL) is based on self-amplified spontaneous emission (SASE) for the generation of ultrashort pulses in the soft to hard X-ray spectral regions, and is driven by a superconducting linear accelerator (linac) with a maximum electron beam energy of 17.5 GeV [Alt06, Alt11, DL13]. Three undulator beamlines serve six scientific instruments:

- **FXE** for studies of dynamic processes in the fields of liquid chemistry and solid state systems
- **SPB/SFX** for single-particle, cluster and biomolecular imaging
- **MID** for studies and imaging of material dynamics on time and length scales inaccessible so far
- **HED** for studies of material under extreme conditions
- **SQS** for studies of small quantum systems by means of gas phase spectroscopy of atoms, ions and molecules
- **SCS** for coherent scattering and photoelectron spectroscopy using soft X-rays

All instruments will allow for time-resolved experiments. A precise knowledge about the temporal delay between pump and probe pulses is therefore crucial for a correct interpretation of the data acquired in those experiments.
The X-ray source is based on a large-scale facility with a total length of 3.6 km, hence a timing jitter between the X-ray and optical pulses is unavoidably present. European XFEL's advanced feedback techniques (based on its superconducting linear accelerator and in conjunction with all-optical synchronisation schemes for the involved laser systems) allow to reduce this timing instability down to the order of a few tens of femtoseconds [SGB+15]. For single-digit femtosecond time resolution, a cross-correlation measurement at or close to the sample position in a user experiment is mandatory and will allow for post-sorting of the acquired experimental data, see e.g. [HCB+13].

This project has received funding from the *European Union's Horizon 2020 research and innovation programme* under grant agreement No 654220

1.2 The FXE Scientific Instrument at the European XFEL

The FXE ("Femtosecond X-Ray Experiments") scientific instrument aims at time-resolved investigation of ultrafast processes in liquid and solid states, and potentially also gaseous samples. The main research focus is chemical dynamics on the molecular level and dynamics in condensed matter systems.

For this, the FXE instrument exploits the short X-ray pulse duration of a few to tens of femtoseconds together with several optical lasers which produce visible light and near-infrared pulses with a duration of tens of femtoseconds, thus enabling time-resolved pump-probe experiments.

X-ray techniques to be applied are various kinds of diffraction (Bragg, powder, amorphous) and spectroscopy. In spectroscopy, the use of X-ray emission spectroscopy (XES) is enabled by two different types of spectrometers ("Johann"-like and "von Hamos"-like), while for X-ray absorption spectroscopy (XAS) the photon energy will be tunable around element-specific absorption edges which can be selected in the range of 5 keV to 20 keV.

Upstream of the sample environment the X-ray beam passes several components and subsystems for diagnostics allowing to adjust the beam parameters to the requirements of the current experiment. In Fig. 1.1, the entire instrument is shown within the experiment hutch, while the components installed in the tunnel are omitted. In the figure, the beam enters the instrument from the lower right and first passes an imaging unit (labelled BIU1 in the figure) for position measurements and a spectrum analyser (SA1). After a slit assembly, it then enters the location which is foreseen for the timing tool installation (TAD, marked with the rightmost orange arrow in the figure). At this location, the X-ray beam is supposed to have constant parameters, as the adjustments for the user experiment are only made subsequently. This allows for a robust implementation of a timing tool. In fact, there is a diamond grating installed upstream in the tunnel, which allows to measure the X-ray/optical arrival time using the first diffracted order, and thus, the measurement is non-invasive to the main beam, i.e. the zeroth order is transmitted through the grating, for the experiment. Here the liquid jet needs to be operated in vacuum, which makes requirements more stringent, as will be discussed below. Additionally, this location is around 6 m away from the sample environment, therefore the required optical laser beam transport may introduce slow drifts. In order to mitigate the influence of thermal drifts the complete X-ray and laser optical branch is covered and equipped with a precision air conditioning system. After the timing tool location, the X-ray beam passes an attenuator assembly (SAA), an intensity monitor (IPM1) and another imaging unit (BIU2) before it enters the compound refractive lens system (CRL) for setting the final focus for the experiment. Before the beam leaves the vacuum system through a diamond window (DW) to the ambient or helium atmosphere sample environment (see the inset of the figure), a final imaging unit (BIU3) and another slit assembly (SL2) is passed. The detector for scattering experiments is designed in such a way that the beam can pass onto another optical table, where additional diagnostic devices are

This project has received funding from the *European Union's Horizon 2020 research and innovation programme* under grant agreement No 654220

installed, such as another spectrum analyser (SA2), an imaging unit (BIU4) and another intensity monitor.

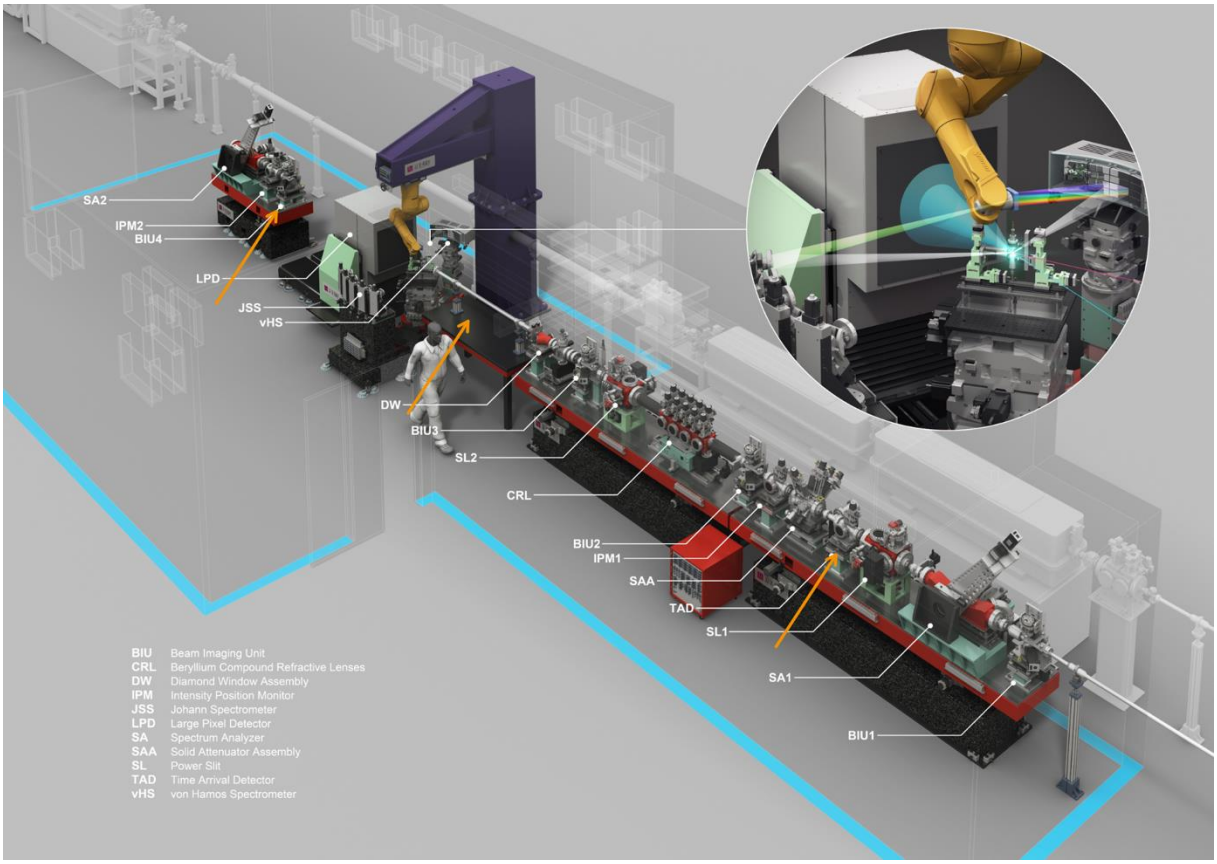

Figure 1.1: Artistic overview of the "Instrument for Femtosecond X-ray Experiments" (FXE) at the European XFEL, including optical components and experimental sections. The X-ray beam is coming from the lower right. The inset shows a close-up of the sample environment, where precisely timed X-ray and optical laser pulses interact in the target. The optical beam can be provided by two laser systems installed in two adjacent laboratories. The orange arrows point to possible locations for the X-ray/optical laser pulse relative arrival time measurement.

The optical laser is coupled into the experiment hutch from an adjacent laboratory roughly 1 m in front of the sample stack, where an optical table provides space for laser diagnostics, beam forming and wavelength conversion. This optical table, being very close to the sample, is also suited for the operation of a liquid jet-based timing tool, yet limited to spectroscopy as the scattering in the liquid jet will spoil the actual, subsequent measurement. For liquid scattering experiments, it may be feasible to install the timing tool closely behind the detector on the last optical table (marked with the leftmost orange arrow in the Figure 1.1). For a certain class of experiments, it might even be feasible to measure the timing *in-situ*, i.e. within the liquid jet used for the actual sample delivery of the experiment. In all cases, the jet is operated in ambient conditions or a helium atmosphere, which makes a technical

This project has received funding from the *European Union's Horizon 2020 research and innovation programme* under grant agreement No 654220

implementation less demanding. On the other hand, at those locations, the timing tool needs to be flexible enough to accept different focus sizes from µm to hundreds of micrometres and attenuation setpoints of covering orders of magnitude of the X-ray beam intensity. Since a change of these parameters will be requested frequently, the timing tool implementation will require a large extent of automation to cope with these changes.

1.3 Time Structure of the European XFEL

In superconducting cavities, the accelerating field can be sustained over a long duration due to low losses and high quality factors as compared to normal conducting cavities. At the European XFEL, the maximum pulse duration of the radio frequency (RF) field is 600 µs, in which a maximum number of 2700 electron bunches with an intra-train repetition rate of 4.5 MHz can be accelerated, i.e. the X-ray pulse separation is 222 ns. In addition, there are several discrete settings for the intra-train repetition rate to reduce it from 4.5 MHz down to ~100 kHz with an accordingly reduced number of maximum pulses. This sequence of electron bunches and X-ray pulses is also called pulse-train. The repetition rate of the pulse-train is 10 Hz, which results ultimately in a so-called burst mode time structure or "bunch pattern" or "pulse pattern", and is depicted schematically in Fig. 1.2.

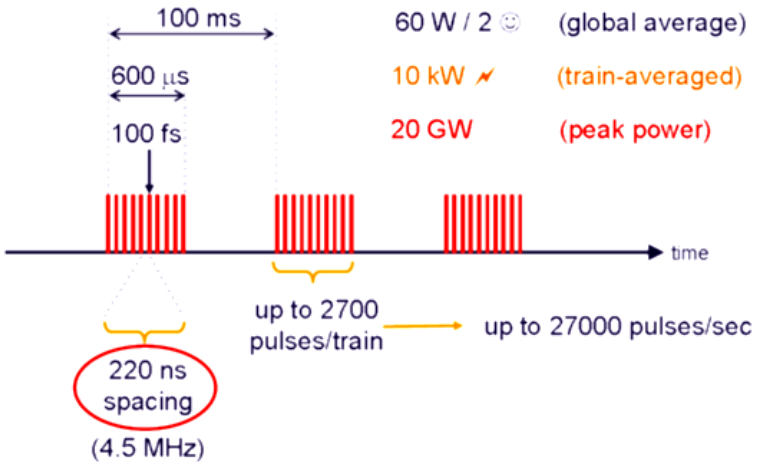

Figure 1.2: Pulse pattern and time structure of the European XFEL.

The high intra-train repetition rate of up to 4.5 MHz will allow for efficient data acquisition, while the several hundreds of microseconds pulse-train duration allow for studies of microsecond dynamics within one pulse-train, but imposes challenges on detector technology at MHz readout frequencies, as well as data transfer, data processing and data storage, see e.g. [BAG+16]. In particular, this affects the online analysis of the retrieved X-ray/optical laser relative arrival time timing tool data and its incorporation into the online data provided to the user during the experiment.

This project has received funding from the *European Union's Horizon 2020 research and innovation programme* under grant agreement No 654220

1.4 ELI Beamlines

The Extreme Light Infrastructure (ELI) is a European project forming a pan-European Laser facility to design and commission the most intense lasers in the world for fundamental and applied research, as user facilities. ELI Beamlines is located in Dolní Břežany, Czech Republic, and is one of three ELI facilities, the other two are in Szeged, Hungary (ELI Attosecond) and Magurele, Romania (ELI Nuclear Physics). ELI Beamlines is currently the largest scientific project in the Czech Republic coordinated by the Institute of physics (FZU) of the Czech Academy of Sciences.

The realization of the ELI Beamlines project started in 2012. This project is a part of the European plan to build a new generation of large research facilities selected by the European Strategy Forum for Research Infrastructures (ESFRI). The main goal of ELI Beamlines is to build one of the most advanced laser resources in the world and implement research projects covering the interaction of light with matter at intensities many times higher than the currently achievable values. ELI Beamlines will produce ultra-short laser pulses of a few femtoseconds (10^{-15} s) duration at the peak power of up to 10 PW. Technologies of ELI Beamlines will enable creation of new techniques for time-resolved spectroscopy, scattering, and diffraction techniques, medical imaging, display, diagnostics, and radiotherapy, tools for design, development, and testing of new materials, improvements of X-ray optics among other. ELI Beamlines will also be an attractive platform for educating a new generation of scientists.

Comprehensive overview of the various laser and experimental technologies is too broad to be presented here (see the webpage of the project [ELIWEB]), for the subjects touching the PUCCA work package the most relevant instrument development will be taking place in Experimental Hall 1 of the ELI Beamlines facility. The different secondary light sources in the E1 hall will be driven by the ELI Beamlines L1 laser, which is going to be providing ~15 femtosecond pulses of up to 100 mJ at a repetition rate of 1 kHz. The primary laser power will be utilized to create three principal kinds of pulsed photon sources: sources spanning the spectrum from ~190 nm ultraviolet to multi-micron infrared, as well as THz wave sources, by nonlinear light conversion of the primary infrared pulse - these will serve also as auxiliary sources, extreme UV source of up to ~100 eV in energy by high harmonic generation in a gas jet (HHG source), and a 4π point source of hard X-rays (5-20 keV) from laser-induced plasma interaction in a liquid metal jet filament (PXS source). All sources but the PXS source will be capable of providing pulse lengths of a few tens of femtoseconds, in the case of the PXS the expected pulse length will be on the order of a few hundred femtoseconds long.

Several experimental endstations are being developed for the E1 hall (see Figure 1.3), these will be covering the area of atomic and molecular science and coherent diffractive imaging (MAC endstation), magneto-optical ellipsometry (ELIps endstation), time-resolved X-ray experiments (TREX endstation at the PXS source), time-resolved optical spectroscopy,

This project has received funding from the *European Union's Horizon 2020 research and innovation programme* under grant agreement No 654220

including stimulated Raman scattering (SRS endstation). Due to the fact that these photon sources are all directly driven by the primary laser light and are generated in close proximity, major sources of jitter are inherently avoided compared to accelerator driven FELs, nonetheless - due to the potentially relatively long travel path between the probing and pumping beams that may magnify the deleterious effects from local vibration sources (e.g., pumps) - a timing jitter on the order of tens of femtoseconds may be expected.

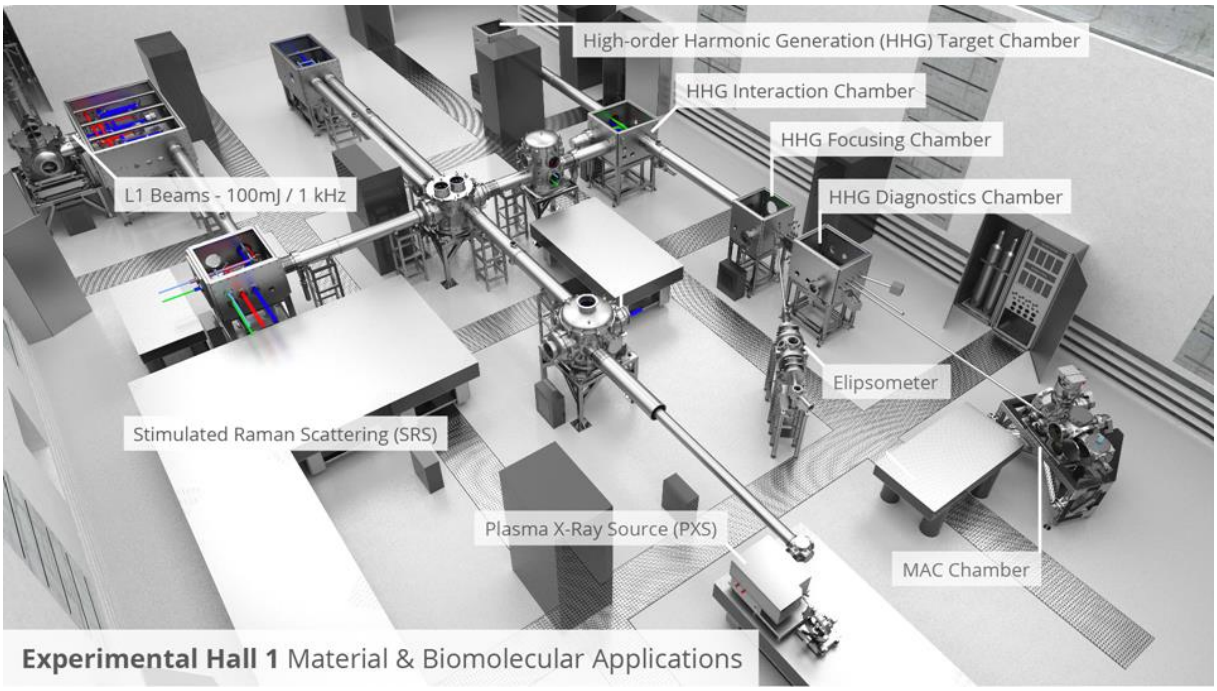

Figure 1.3: Artistic view of the secondary sources and end-stations of the Experimental Hall 1 at ELI Beamlines.

This project has received funding from the *European Union's Horizon 2020 research and innovation programme* under grant agreement No 654220

2 Objectives

The EUCALL project description states: *"European XFEL is developing 4.5 MHz repetition rate X-ray/optical diagnostics and has already acquired experience in exploiting such high repetition rates at SR sources. XFEL experiments at LCLS and SACLA sought to reveal dynamic effects on the femtosecond level, and XFEL has also contributed to the 100 Hz development of a sub-10 fs timing tool at LCLS. Within this project XFEL will develop schemes to measure the precise arrival time of pulses from a distant light source (with respect to an independent closer light source) at MHz repetition rates based on fast liquid jets for fast sample exchange on a shot-by-shot basis. This effort aims to exploit the energy range from about 5 – 20 keV, but also throughout the UV-vis-NIR range. [...] ELI joins these timing tool efforts by developing a similar liquid jet based tool to measure the arrival time between two independent laser sources (of which one may serve as an X-ray plasma source)."*
Based on this, the requirements and capabilities of the liquid jet used for the realisation of the measurement of the relative arrival time of EUV, soft and hard X-ray pulses relative to an optical laser are defined.

2.1 Liquid Jet Timing Tool Requirements for Tender and Hard X-rays

The requirements for a liquid sheet-based timing tool (and/or sample delivery system) for hard X-ray applications are the following:

- linear flow speed of the liquid of about 100 µm/µs to accommodate the high intra-train repetition rate (4.5 MHz) of the European XFEL, such that the sample volume is replaced for each pulse in the train;
- variable sheet thickness in the range of 0.1-1 µm (this depends on the detection scheme, transmissive schemes may suffer from loss of time resolution at thicknesses above 10 µm);
- the width of the flat, unobstructed part of the sheet is optimally 0.5-2 mm;
- flat, uniform surface with no ripples or waves;
- running water and different alcohols (ethanol tested);
- closed loop operation (reflow the sample);
- capability of operation in vacuum is desirable;
- motorized control of jet position relative to X-ray/optical beam and focus (3 axis)
    - corresponding motion of catcher assembly;
- full integration into the facilities' data acquisition and control system (Karabo at the European XFEL, Tango at ELI);

This project has received funding from the *European Union's Horizon 2020 research and innovation programme* under grant agreement No 654220

- easy maintenance;
- online monitoring of the injection with an optical camera;
- possibility for double use as means for sample introduction
    - for specific cases, this would mean that simultaneous X-ray scattering application could be used along with timing purposes.

The main requirements for the timing tool to be utilized for hard X-rays applications stem primarily from the high repetition rate of the XFEL source, which then result in the need for high rate of sample replacement, - i.e., high liquid speed. However, many applications at the hard X-ray beamlines can be performed outside of vacuum chambers, in air or in protective atmosphere - this puts less demand on the effort to minimize the volumetric flow rate in cases where the liquid is not used simultaneously as a (limited) sample.

2.2 Timing Tool Based on Microfluidic Liquid Sheet Jet

For applications with soft X-ray and extreme UV radiation vacuum environment is always required for the experiments, in contrast to hard X-ray applications. This mostly means that the vacuum environment needs to be protected from the operation.

In recent years, liquid jet systems capable of delivering extremely thin jets of the order of one micrometre has been developed [DWS+08, TKD+14] which is capable of operation in such conditions. The system is based on the utilisation of the technique of gas dynamic virtual nozzle (GDVN) where gas pressure and flow is utilized to compress and elongate the liquid stream into a jet of a few micron to sub-micron diameter, one to two orders of magnitude thinner than a regular Rayleigh jet produced by a simple orifice would allow. For sample introduction purposes a major advantage of these micro-liquid jets is the relatively small liquid consumption rate, on the order of hundreds of microliters per hour. Recently the technique has been modified to produce also flat liquid sheets that could be utilized for the purpose of a liquid jet based timing tool. The liquid sheet of the microjet can serve as a moving target for characterizing the X-ray pulses and the arrival time.

The requirement for the liquid microjet sheet-based timing tool are the following:

- The surface of the sheet should be uniform, with minimum roughness.
- The linear speed of the flow of liquid (water) should be approximately around 100 µm/µs to accommodate the shot-to-shot spacing of the European XFEL shown in Figure 1.2, 220 ns (4.5 MHz rep rate) of 2-100 fs X-ray pulses (600 µs pulse per train with up to 2700 pulses per train with 0.1 second separation / 10 Hz rep rate of the pulse train). For the kHz repetition rate of X-ray/XUV sources at ELI Beamlines, the flow velocity may be slower.

This project has received funding from the *European Union's Horizon 2020 research and innovation programme* under grant agreement No 654220

- The volumetric flow rate should be as low as possible, desirably less than circa 100 µL/min, to enable operation in deeper vacuum. The estimates of the volumetric flow rates are shown in Table 2.1. The total flow of the supporting gas envelope needs also to be taken in consideration, since it might easily overwhelm the vacuum pumping system.
- The clear (uniform) width and the length of the surface of the sheet should be about 100 µm to accommodate a few hundreds of femtoseconds jitter of the X-ray pulse (see below).
- The thickness should be less than 1 µm. The thickness sets the flow rate of the liquid, the thinner the jet, the better for the vacuum system. For the application as a timing tool, only the surface quality is important, the thickness is of less relevance. It can be as thin 100 nm.
    - However, for some other applications, for instance in water radiolysis measured by transient absorption at low X-ray flux such as 5 − 20 keV plasma X-ray sources planned at ELI Beamlines, thicker jets would be of interest with the thicknesses above 1 µm.

The estimates of the flow rates for 1 µm and 0.2 µm thick sheets for the velocity of the liquid equal to 100 µm/µs are presented in Table 2.1.

Table 2.1: Estimates of the parameters of the microjet sheet for the X-ray timing tool.

Width		**thickness**		**velocity**	**volumetric flow rate**		
µm	M	µm	m	m/s = µm/µs	m^3/s	cm^3/s = mL/s	mL/min
100	1×10^{-4}	1.0	1×10^{-6}	100	1×10^{-8}	0.010	0.60
100	1×10^{-4}	0.2	2×10^{-7}	100	2×10^{-9}	0.002	0.12

2.3 Detection Scheme Considerations

2.3.1 Spatial Time Encoding

One possible method for the detection is based on the change of reflectivity of the surface of the liquid (usually water) sheet. As mentioned already above, X-ray/optical cross-correlation has been shown to be effective for the case of solid substrates [GAB+08, MCW+08, Dur12, KTS+12, HCB+13, DBP+14, STO+15, EBP+15], while the usage of liquid water and of other liquids has been so far investigated to a lesser degree [HGR+10]. It is generally expected that the reflectivity of the water surface will rapidly change with the impact of an X-ray pulse, since it is well known that spectral properties of water do change already during the first tens of femtosecond during pulse radiolysis [OKS+11, YKK+11]. Nonetheless, the exact dynamics will need to be investigated to achieve comparable level of timing precision.

This project has received funding from the *European Union's Horizon 2020 research and innovation programme* under grant agreement No 654220

For reflection based detection, the thickness of the sample sheet is of small significance. However, the width ***W*** of the liquid flat sheet defines several parameters with respect to time window and temporal resolution(see Figure 2.1). In a geometry where the X-ray beam and the probing optical laser beam are perpendicular, the optical laser pulse arrival time t_1 will be mapped directly on the planar image of the reflection of the optical laser beam as $L = c \cdot t_1$ (the time t_1 is the period of delay of the laser pulse after the first moment of interaction of the X-ray with the liquid sheet, ***c*** is the speed of light in vacuum). For the purposes of the experiment, a more practical "time zero" would be the moment of central overlap of both pulses (where $L = 0.5 \cdot W \cdot \cos \varphi$) , but the selection may depend on which pulse is to come earlier on the sample in the particular study.

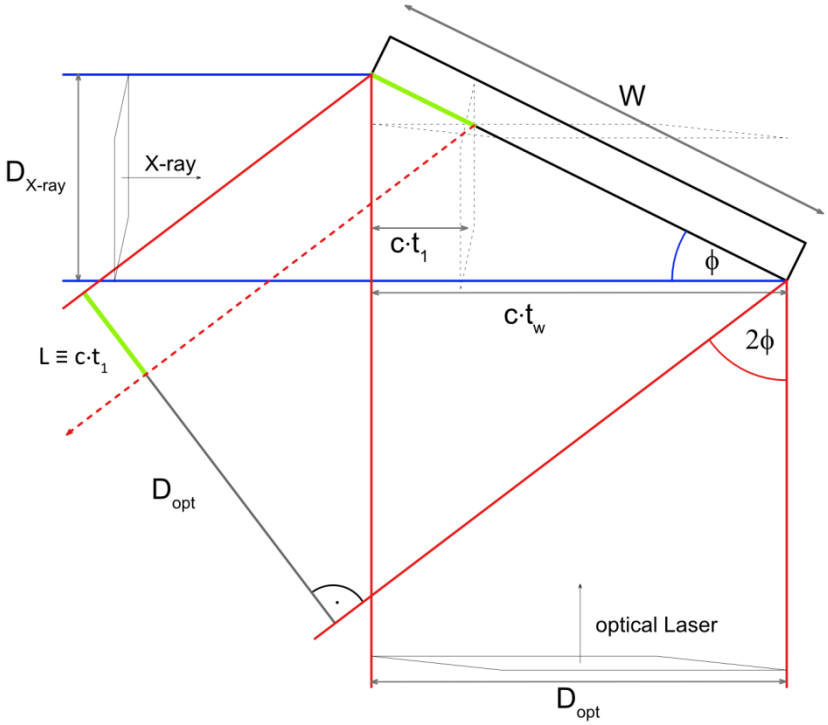

Figure 2.1: Geometrical considerations for the usage of the liquid sheet for spatial-based time encoding.

The observable time window will depend on the angle ***φ*** of incidence of the X-ray beam with the liquid sheet. The entire maximum span of the time window to investigate the timing jitter is given by $t_w = W \cdot c^{-1} \cdot \cos \varphi$.

For example, if the sheet width is ***W* = 100 µm** and the angle of laser beam incidence is ***φ* = 22.5°** (under this circumstance the reflected laser beam has a 90° - 2***φ*** = 45° angle with the incoming X-ray beam), then the time window is t_w **= 308 fs**. The relatively sharp angle will either require that the X-ray pulse diameter is either equal to $W \cdot \sin \phi = D_{X\text{-}ray}$ **= 38.3 µm**, or that only a smaller portion of the same width of the X-ray pulse is imaged, which potentially can be a split-off beam of the main X-ray beam [KOT+16]. The imaging laser beam diameter

This project has received funding from the *European Union's Horizon 2020 research and innovation programme* under grant agreement No 654220

then must be more than $W.\ cos\ \varphi = \boldsymbol{D_{opt}} = \mathbf{92.4\ \mu m}$ wide. A limit on the time resolution will then be determined by the pixel density of the imaging system. Subsequently the imaged area / line of D_{opt} is going to be magnified by optics onto either a 2D camera chip or onto a 1D pixel array. A time resolution per pixel can then easily be calculated. Dividing the time window by the number of the illuminated pixels, e.g. 308 fs / 100 px yields 3 fs per pixel.
However, the actual radiation physics of the change of reflectivity on the surface and instrumental sources of instability will certainly introduce signal dispersion that will degrade the timing resolution, experience with similar systems on solid samples had a 5 - 10 fs (RMS) residual timing jitter [DBP+14, STO+15].

2.3.2 Spectral Time Encoding

Another possible method for relative X-ray/optical timing measurement by exploiting a change of optical properties of a material is the spectral encoding technique, which schematically is shown in Fig. 2.2 and described in the EUCALL project description as Task 7.1.2. In this method, the optical probe pulse is a spectrally broadband white light ("supercontinuum") pulse, which is generated either in a crystal or via filamentation [BKL+95] from the 800 nm optical pump-probe laser. Due to the chirp of the pulse, i.e., the different velocities of different spectral components resulting from the generation process, a low-order polynomial mapping between time and wavelength is established (see, e.g., [HCB+13, BHW+14] where - in these studies a sub-10 fs timing resolution was achieved on solid samples at LCLS). Overlapping the supercontinuum with the X-ray pulse in a liquid jet or thin solid samples, as it is realised for established timing tools at low repetition rates, leads to a change of the complex refractive index. Thus amplitude and phase of the transmitted optical spectrum are modulated at a particular wavelength depending on the instant of overlap. Hence, the spectral location of the feature can be translated into a relative arrival time of the pulses.

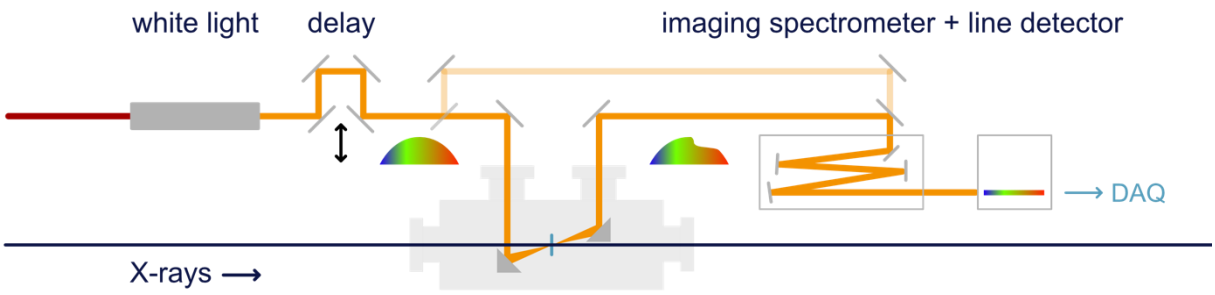

Figure 2.2: Sketch of the spectral encoding scheme for the measurement of the relative arrival time between X-rays and optical pulses.

This project has received funding from the *European Union's Horizon 2020 research and innovation programme* under grant agreement No 654220

As can be seen on the sketch of the method in Figure 2.2 above, the pulse arrival can be identified through an increased optical absorption of a portion of the spectrum of the transmitted chirped pulse. Since the introduced chirp is a known parameter, the specific wavelength at which the drop-in transmittance occurs carries the information about the delay between the X-ray and optical pulses. The advantage of this technique is two-fold: first, the temporal window can be tailored by applying more or less chirp to the probe pulse for either covering a larger time window in the order of several picoseconds or by reducing the window to increase the temporal resolution (which, however, is limited by other factors as well). Second, from a technical point of view, spectral encoding is favoured over spatial encoding at the European XFEL, since only a 1D (or "line") detector is required in comparison to spatial encoding and hence it can be realised at the 4.5 MHz high intra-train repetition rates as mentioned above.

This project has received funding from the *European Union's Horizon 2020 research and innovation programme* under grant agreement No 654220

3 Methods, Experiments and Results

3.1 Flat-Sheet Colliding Jet

The first liquid jet system under investigation is a commercial device developed and manufactured by Microliquids GmbH, Göttingen (http://microliquids.com), since it promises to meet the requirements described above. It is based on the phenomenon that upon collision of two round, laminar jets under an angle a stable flat sheet is formed, as sketched in Fig. 3.1. Depending on the angle and positioning of the nozzles with respect to each other, their diameter and their individual pressures the thickness, flatness, shape and stability of the sheet can be influenced and controlled to some extent. Typically, the width of such a sheet is between 0.5 mm and 1 mm while the length, i.e. the size in the liquid flow direction, of the flat part of the sheet is a few millimetres.

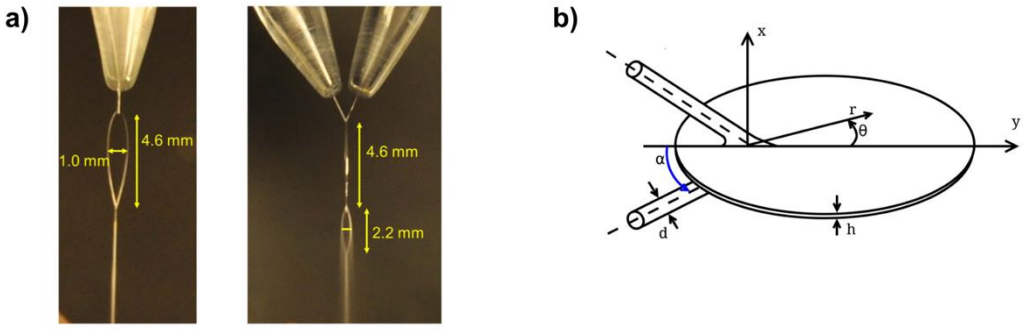

Figure 3.1: a) Photographs of a liquid flat sheet from two orthogonal directions showing the formation of a first sheet (left picture) and a second, smaller one. b) Sketch of the flat sheet with notation used, taken from [EQF+15].

The system shown in Fig. 3.2 is equipped with several manual and motorised translation stages which provide the required degrees of freedom for alignment of the nozzles. Moreover, the system is prepared to be used in vacuum (with pressures of around 10^{-3} mbar) and therefore mounted on a DN100 CF flange. The complete jet assembly can be moved using motorised translation stages by ±10 mm in all three dimensions to allow an optimum placement of the jet once integrated into the experiment or sample environment. The delivery of the liquid to the nozzles is equipped with individual pressure regulators, providing another possibility for fine-tuning the flat sheet. In addition, the pipes for the liquid are installed inside another pipe, where another liquid can be flown for tempering the sample liquid using an external heater or cooler. Finally, a catcher assembly (not depicted here) is used to collect the liquid and allows for reflowing it, which is in particular important when such a jet is not only used in a timing tool configuration, but for actual sample delivery.

This project has received funding from the *European Union's Horizon 2020 research and innovation programme* under grant agreement No 654220

The pressure system is consisting of a commercial HPLC pump (Shimadzu LC-20AP Prominence) and pulsation dampeners.

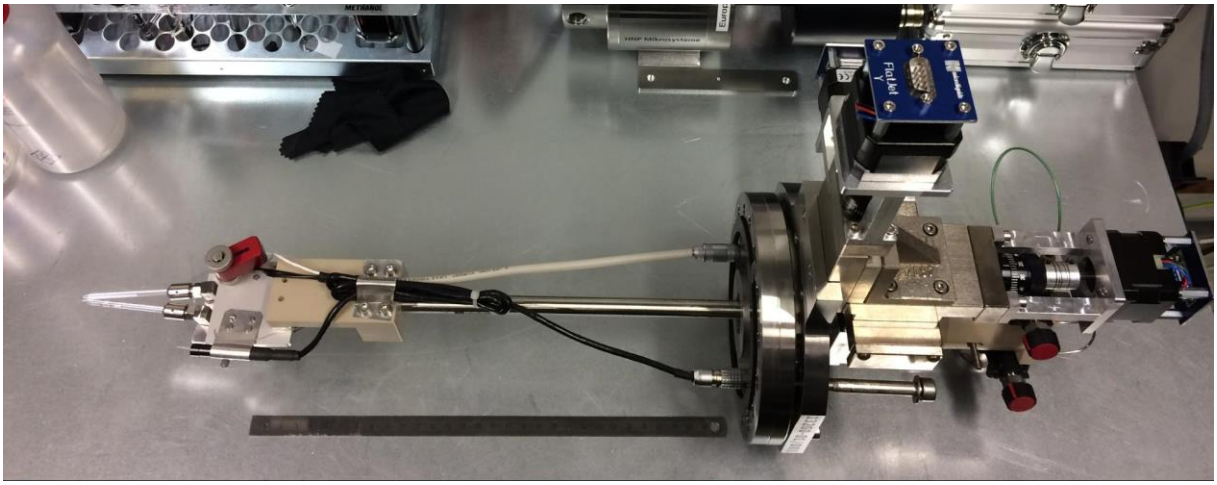

Figure 3.2: Photograph of the colliding flat-sheet jet assembly. On the left, the two nozzles installed at an angle are visible, together with one motor for remote optimisation of the sheet and a diagnostic camera. On the right, the motorised manipulator and individual pressure regulators for the nozzles can be seen. The central rod includes the possibility for tempering the liquid. The vacuum-ready assembly is based on a DN100 CF flange. The catcher assembly and the pressure system are not shown in the picture.

3.1.1 Flatness and Thickness Measurements

The flatness and the thickness of the sheet are two important parameters and were the first to be analysed. The basis for this is a technique called confocal achromatic imaging, sketched in Fig. 3.3, where the light of a white source (typically an LED) falls onto a chromatic lens, such that the focal planes for different wavelength have a different distance to the lens. When light is reflected from a surface placed at a certain distance from the lens, the light with the corresponding wavelength is reflected and can be analyses using a spectrometer. If light is also reflected from the back surface of a thin, optically transparent sample, such as an liquid flat sheet jet operated with water, interference occurs which thus can be used to analyse also the thickness of the sample in a contactless way. For the measurements discussed below an commercial device (Polytec/STIL TopSens CCS Prima with optical pen CL0-MG140) is used, which allows for a thickness range of sub-5 µm up to 100 µm at a working distance of approximately 2.7 mm.

This project has received funding from the *European Union's Horizon 2020 research and innovation programme* under grant agreement No 654220

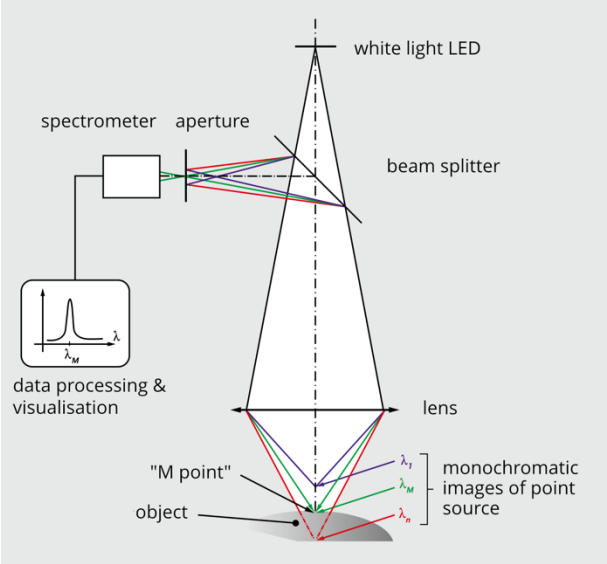

Figure 3.3: Principle of confocal chromatic imaging, being the basis for contactless distance and thickness measurements.

Figure 3.4 shows the results of a thickness measurement series, where the jet is equipped with nozzles of 128 µm diameter and operated at different volumetric flow rates of 60 ml/min, 70 ml/min and 80 ml/min. Clearly, as can be seen in the left graph, for all flow rates the thickness reduces from tens of micrometres to less than 10 µm over a distance of 15 mm along the liquid flow direction ("*y*" direction in Fig. 3.1b) in the sheet. The right graph of Fig. 3.4 shows the thickness of the jet across the sheet ("*x*") for selected flow rates and *y*-positions on the sheet. Notably, the sheet is not uniformly flat over its extent in *y*-direction, but exhibits a certain curvature, which changes from convex to concave the further away from the liquid interaction point and the thinner it gets. Thus, there is only one particular point where the surface is flat, which will have a particular thickness depending on the nozzle size and flow rate. This result has to be considered when operating the timing tool in the spatial encoding geometry, as explained in Section 2 above. For this particular configuration of the liquid jet system, the optimum conditions are a flow rate of around 80 ml/min., with a resulting thickness of ~5 µm.

To produce thinner sheets with the colliding jet technique, nozzles with smaller diameter can be used, which however may have negative consequences on the speed of the jet, as lower flow rates may be required. It is planned to investigate this in the near future.

For permanent operation of a liquid jet timing tool, the possibility of diagnosing the thickness of the jet is desirable, such that integration of an optical pen sensor should be considered.

This project has received funding from the *European Union's Horizon 2020 research and innovation programme* under grant agreement No 654220

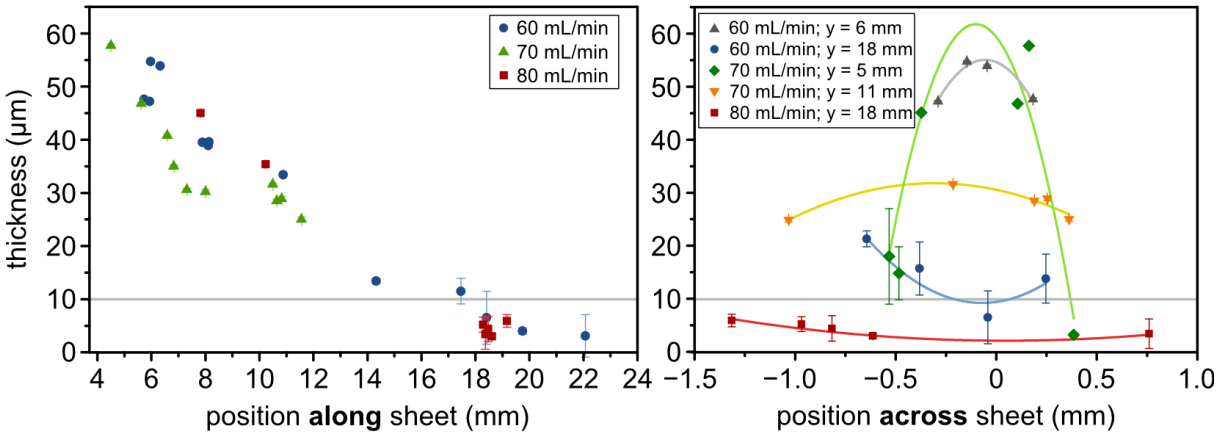

Figure 3.4: Thickness (a) and flatness analysis (b) of the colliding jet as function of the position along ("y") and across ("x") the "leaf".

3.1.2 Measurement of the Flow Speed of the Jet

The flow speed of the liquid jet is an important figure of merit for the MHz intra-train repetition rate of the European XFEL. Ideally, the complete interaction volume of the X-rays and the optical laser pulse should be replaced from shot to shot. In case of the spectral encoding geometry a reasonable laser focus size is 25 µm, which would require a linear flow speed of 113 m/s for a repetition rate of 4.5 MHz, i.e. bunch spacing of 222 ns.

To measure the flow speed of a liquid jet, we distort the sheet with an intense ultrashort laser pulse and then track the development of this distortion in time using a high-speed camera. The geometry is sketched in Fig. 3.4 a). The back-illuminated liquid jet is imaged using a microscope objective onto the sensor of a Photron FastCam SA4, which is capable of recording up to 500000 frames per second (fps) with a minimum shutter speed of 1 µs. For the measurement, the laser pulses were distorting the liquid sheet at kHz repetition rate, such that a single impact could be tracked with the fast camera.

This project has received funding from the *European Union's Horizon 2020 research and innovation programme* under grant agreement No 654220

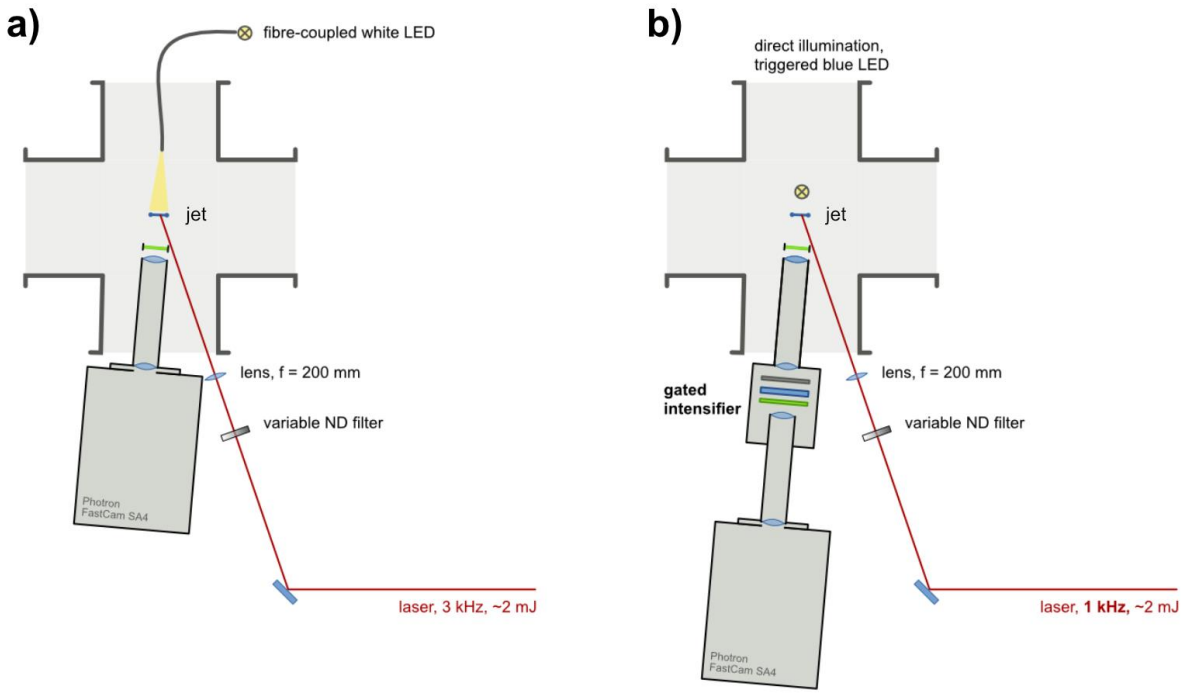

Figure 3.5: Schematic top-view of experiments to determine the flow speed of a liquid jet indirectly using an ultrashort intense laser pulse. In a) a high-speed optical camera is used to film the laser induced distortion of the jet directly while in b) a gated image intensifier is used to improve temporal and spatial resolution.

In a first series of measurements we recorded the development of a laser-induced distortion of the sheet for different laser pulse energies and again for the three volumetric flow rates of 60 ml/min, 70 ml/min and 80 ml/min. Figure 3.6 shows a series of frames taken from videos which were recorded with 360000 fps and a laser pulse energy of 100 µJ imping the flat sheet (see panel a) in the figure). After 2.8 µs (1/360000 s, i.e. the next frame shown in panel b)) the induced distortion is clearly larger than the impinging laser spot, but hardly any motion can be observed. For later times, as shown in panels c) and d) for ~30 µs and 75 µs after the impact, different propagation lengths and change of the shape of the distortion become obvious. While for the lowest flow rate the shape of the distortion stays practically round while it keeps growing and eventually forms a hole in the liquid sheet, it even breaks up into two fractions for the highest flow rate. This, and the distortion of the branches of the sheet are a clear sign for instability of the jet in this setting. It should be noted that the jet assembly needed to be relocated and realigned in the laboratory where the measurements were carried out, such that the parameters of the sheet may be different from them discussed in the previous section on the thickness and flatness measurements. This underlines again the need for diagnostic measures when the jet is employed as a timing tool in a user experiment. Finally, it is interesting to note that at higher flowrates, another systematic distortion of the branches of the jet is seen, roughly 100 µs after the laser impact

This project has received funding from the *European Union's Horizon 2020 research and innovation programme* under grant agreement No 654220

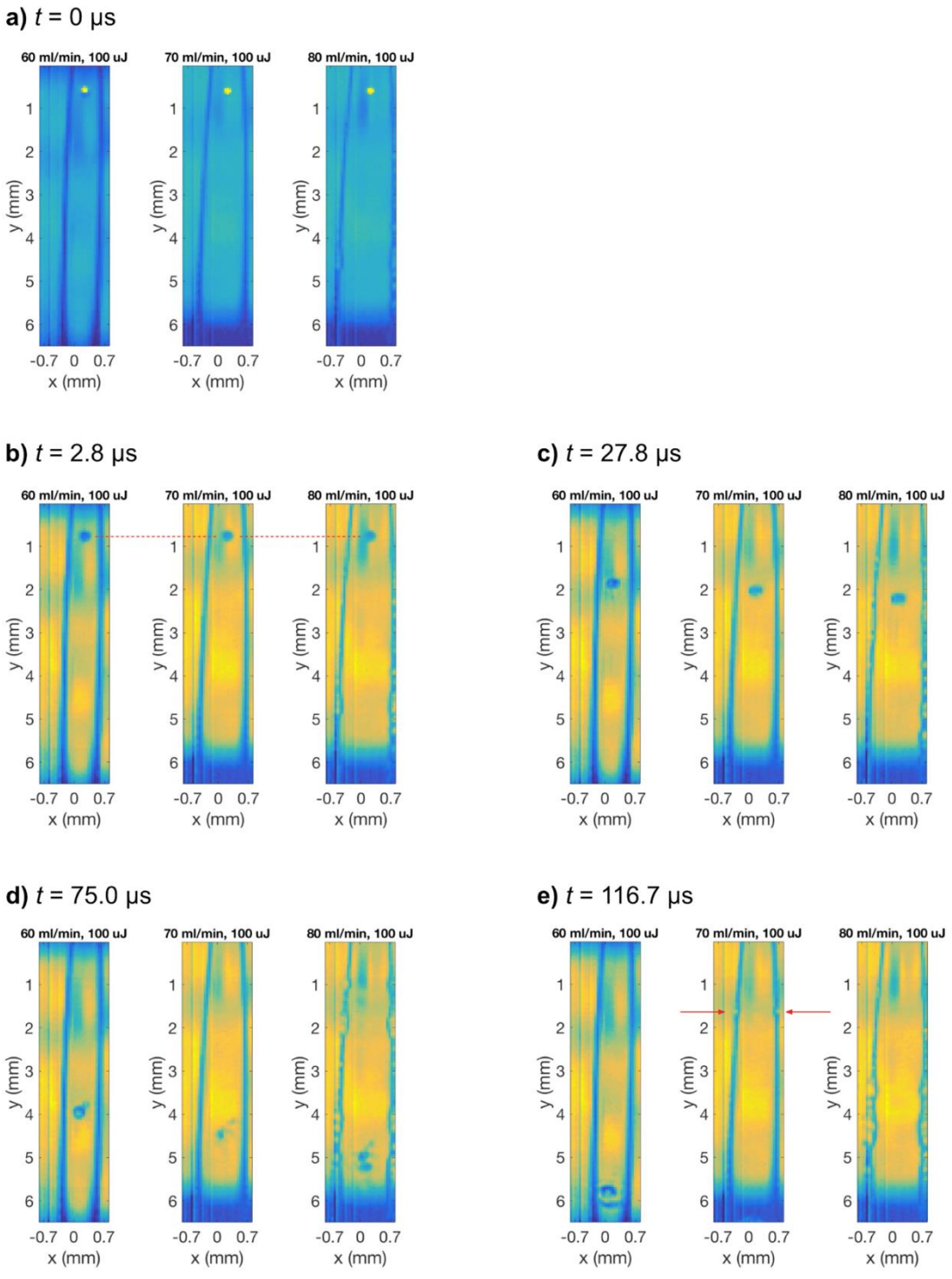

Figure 3.6: Frame grabs from movies of flat jets with different volumetric flow rates recorded at a rate of 360000 frames per second a) at the time of the laser impact on the flat jet, b) after 2.8 µs, i.e. the first frame after the impact, c) after ~28 µs, d) after 75 µs and e) after ~117 µs.

This project has received funding from the *European Union's Horizon 2020 research and innovation programme* under grant agreement No 654220

as depicted in panel e) in the figure.

To calculate the linear flow speed of the jet, for each laser event a background, being the average of 20 frames (corresponding to 56 µs in these measurements) before the laser pulse arrives, is subtracted from each of the first 20 frames following the laser impact for which then the width and the centre of the distortion in the flat sheet is determined.

The result of this analysis for the different pump laser energies and flow rates is summarised in Fig. 3.7 and Table 3.1. Each data point in the figure represents an average of the analysis of 50 consecutive laser events while the line shows the average of all these data points. Notably, all determined speeds are approximately 10% higher than the estimate from the volumetric flow rate $Q = \boldsymbol{v} \cdot \boldsymbol{A}$, where $\boldsymbol{v} = v \cdot \boldsymbol{n}$ is the flow speed along the direction $\boldsymbol{n}$ through a surface $\boldsymbol{A} = A \cdot \boldsymbol{n}$ with the normal $\boldsymbol{n}$. As expected, the speed is not high enough to cope with the maximum intra-train bunch spacing of 222 ns at the European XFEL for a complete replacement of the interaction volume, because the laser spot size will be around 25 µm. It remains to be demonstrated if a replacement of approximately one half is sufficient for effective relative timing measurements, and if faster flowing water jets with a thickness of a few micrometres can be realised. However, since also the intra-train repetition rate European XFEL can be varied, the investigated jets are potentially suitable for all experiments but the ones with the highest repetition rate.

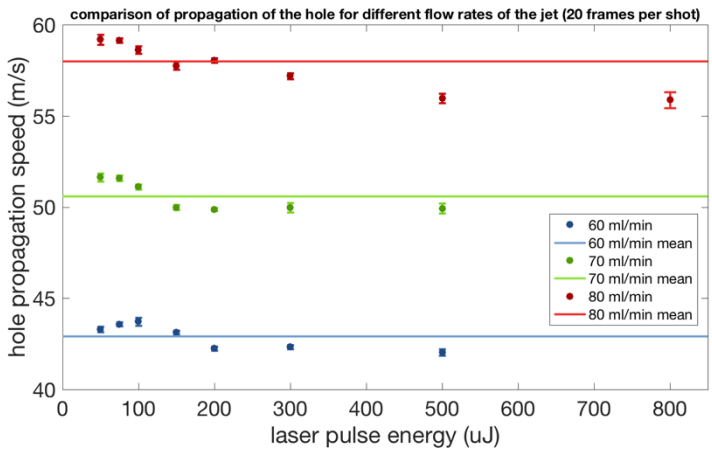

Figure 3.7: Summary of the laser pulse assisted flow speed measurements of the flat sheet for different flow rates. Each data point represents the speed obtained from an average of 50 consecutive laser impacts.

To investigate the distortion directly after the impact of the laser pulse and in particular in between to X-ray pulses with 222 ns spacing, the limitations of the direct imaging need to be overcome. Those include limited time resolution in the order of a few microsecond given by the camera exposure time and frame rate, as well as only limited spatial resolution given by the camera (128 x 32 pixels at 360 000 fps). Therefore, we performed a second series of measurements on the flat sheet liquid jet, where we incorporated a gated image intensifier

This project has received funding from the *European Union's Horizon 2020 research and innovation programme* under grant agreement No 654220

(Hamamatsu C9538-03) into the setup. Such an image intensifier consists of a photocathode which converts incoming photons into electrons, a microchannel plate (MCP) serving as intensifier as the number of electrons is significantly multiplied by showering in the MCP, an accelerating electric field realised as a high voltage between the two sides of the MCP, and a fluorescent screen to convert the electrons back into visible light which can be recorded using the fast camera. This modified measurement setup is sketched in panel b) of Fig. 3.5 and also depicted in Fig. 3.10 below.

Table 3.1: Results of the laser pulse assisted flow speed measurements for different flow rates and nozzle diameters.

80 ml/min, 128 µm nozzles	**SI**	**bunch spacing**
measured	(58.0 ± 1.1) m/s	(12.9 ± 0.3) µm/222 ns
theoretical	51.8 m/s	11.5 µm/222 ns
70 ml/min, 128 µm nozzles		
measured	(50.6 ± 0.8) m/s	(11.2 ± 0.2) µm/222 ns
theoretical	45.3 m/s	10.1 µm/222 ns
60 ml/min, 128 µm nozzles		
measured	(42.9 ± 0.7) m/s	(9.5 ± 0.2) µm/222 ns
theoretical	38.9 m/s	8.6 µm/222 ns
50 ml/min, 100 µm nozzles		
measured	44.3 m/s	9.8 µm/222 ns
theoretical	53.1 m/s	11.8 µm/222 ns

The main advantage of this technique is the greatly improved temporal resolutions as the time, where the high voltage pulse is active, and by this effectively gating the light which falls onto the camera, can be as short as 30 ns, being a factor of about 100 compared to the measurements described above. Furthermore, with an improved imaging system, the spatial resolution could also be improved and the full frame of the camera could be employed. The drawback of the used image intensifier unit is the limited repetition rate of approximately 200 kHz, which required us to use the even lower repetition rate of 1 kHz of the optical laser system. In contrast to the measurements with direct imaging of the liquid sheet, where we can follow the development of the laser-induced distortion for a single shot, we here need to record a number of images for each time delay after the impact.

This project has received funding from the *European Union's Horizon 2020 research and innovation programme* under grant agreement No 654220

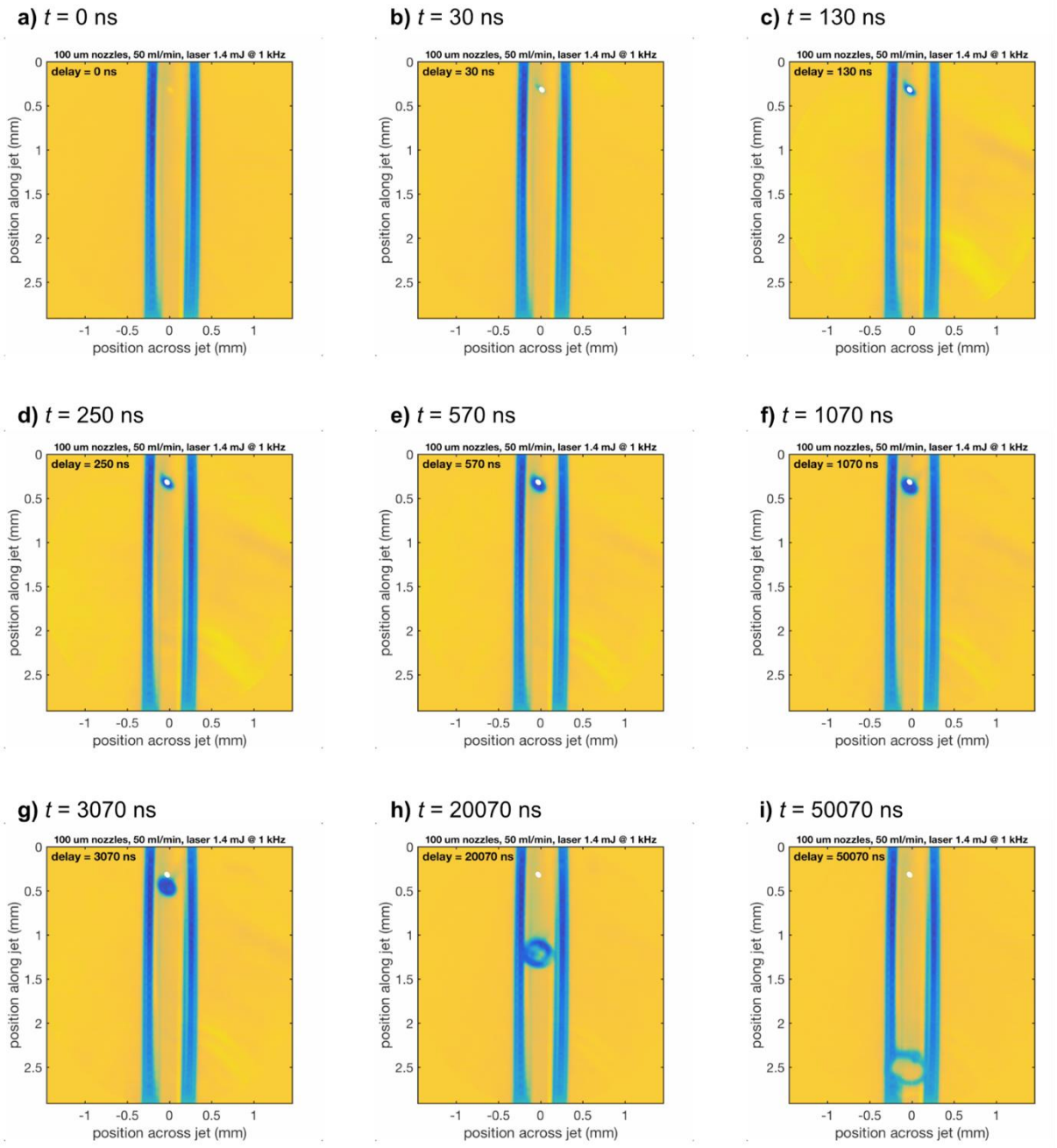

Figure 3.8: Frame grabs of a movie recorded using an gated image intensifier with a gate length of 30 ns. Each frame is an average of 1000 images recorded at different time delays after the laser impact. The white spot b) to i) marks the location of the impact of the laser pulse as shown in a).

An example of such a measurement is shown in Fig. 3.8, where each panel shows an average of 1000 frames (1 second of measurement time) for different time delays, with a background subtracted which was recorded without the jet running. Note that for this measurement nozzles with 100 µm diameter were used with a flow rate of 50 ml/min, which turned out to be the most stable operating point. Since in this measurement we were only interested in

This project has received funding from the *European Union's Horizon 2020 research and innovation programme* under grant agreement No 654220

the speed of the jet and in particular the capabilities of the gated image intensifier unit, we did not measure the thickness of the jet for this configuration.

Due to the lower flow rate the jet is less wide, yet it spans around 500 µm between the branches which is sufficient for all envisioned use cases. After the laser impact, shown in panel a) in Fig. 3.8, the induced distortion by the laser seems to grow on a fast time-scale in the liquid medium, as practically now movement is observed after 30 ns (panel b)) and even 100 ns later (panel c)) as can be seen when compared to the original location of laser impact depicted with the white dot. In panels d) to f) it can be seen that the distortion starts to propagate with the flow of the liquid, and only after approximately 3 µs the distortion of the liquid jet does not overlap with the original impact location (panel g)). After 10 µs (panel h)), a clear, circular hole has developed in the flat sheet, which extends the complete width after 50 µs (panel i)).

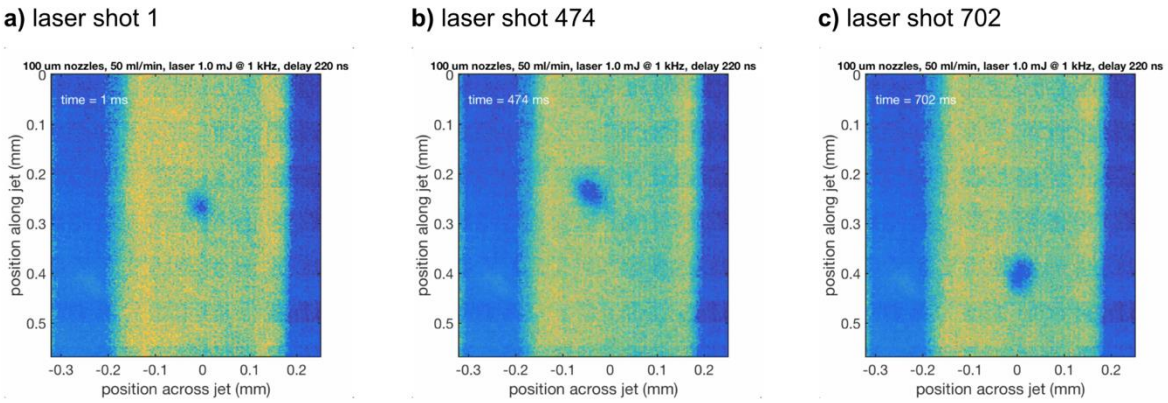

Figure 3.9: Frame grabs of a movie recorded using an gated image intensifier with a gate length of 30 ns at a fixed set delay of 220 ns after the laser impact for different laser shots.

For more insight at the development of the distortion at the time delay when the next X-ray/optical laser pulse pair is arriving, we recorded a number of laser shots at the corresponding time delay of ~220 ns after the first impact. Figure 3.9 shows as examples the first recorded laser impact in panel a) and two other ones after 473 ms and 701 ms. Clearly, the position of the distortion induced by the first laser shot has a different position compared to the one of the first shot by up to 150 µm. Our present explanation for this is a combination of instabilities of the pointing of the laser and the liquid jet itself, but further analysis and additional measurements are required. Specifically, it needs to be determined whether the apparent growth of the distortion discussed in Fig. 3.8 is purely caused by the instability of the distortion caused by averaging or if other mechanisms, like shockwaves or microcavities, cause the distortion to grow faster than it can flow down with the liquid.

This project has received funding from the *European Union's Horizon 2020 research and innovation programme* under grant agreement No 654220

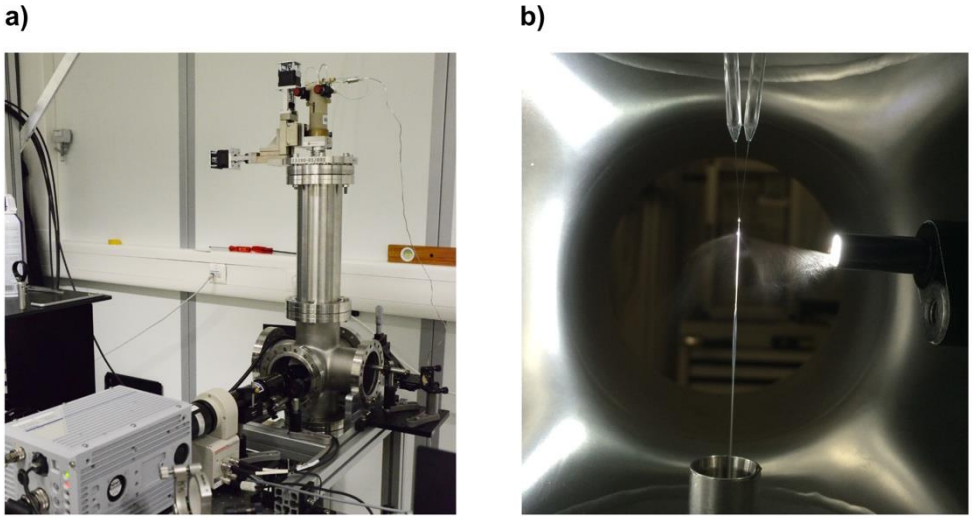

Figure 3.10: Photograph of the setup to measure the jet flow speed with the gated image intensifier unit. In a) the jet is mounted into its vacuum-ready structure in the center of the picture, and the image intensifier and the camera are visible in the lower right. In b) a close-up side-view of the liquid sheet is shown, where the spray of liquid is caused by the near-infrared laser beam coming from the left side. Upon careful observation, also the second leaf is visible (compare Fig. 3.1).

3.2 LCLS Sample Environment Jet

Nozzles that can generate thin liquid columns and sheets are desirable for use in sample delivery systems at soft X-ray and electron sources. A soft X-ray source operating at the oxygen K-edge has a 1/*e* attenuation length of only 500 nm, which is coincidentally, about the maximum usable thickness of a liquid in a 200 keV transmission electron microscope.

Due to the likelihood of nozzle clogging for diameters under 20 micrometres it is advantageous to produce thin liquid targets by starting with larger nozzles then reducing the downstream liquid thickness. This can be accomplished by accelerating the liquid or spreading out the liquid with the application of transverse momentum through colliding jets, converging channels or in this case by a gas dynamic forces.

In cooperation with our partners from the DePonte group at the LCLS X-ray free electron laser facility, a microfluidic sheet device was tested. Prototype microfluidic sheet jets were produced by *Micronit Microfluidics BV* and consisted of three channels converging at the edge of a glass chip. The central channel was 20 micrometres in diameter and the two external channels were approximately 50 micrometres. Three geometries were tested with a convergence half angle of the external channels chosen as either 20, 30, or 40 degrees. The external channels were equal in length and connected to a single port approximately 1 cm from the exit of the chip.

This project has received funding from the *European Union's Horizon 2020 research and innovation programme* under grant agreement No 654220

Testing was carried out in a rough-pumped vacuum vessel at pressures from single Torr (1.3 mbar) to a few tenths of a Torr depending on the gas load. The liquid flow was controlled by pressurized reservoir. The jet was imaged with an external long working distance microscope through a glass port. All tests were carried out with helium used as the gas in the external channels and purified water for the liquid jet.

Figure 3.11: Optical micrograph of a liquid sheet in vacuum produced from a 20 micron orifice. The edge of the nozzle can be seen on the left. Gas-dynamic forces cause the liquid to spread out into a thin sheet.

It was found that the most reliable method to start the nozzle vacuum was to start with a free liquid jet and then increase the pressure in the external channels. As the gas pressure increases, the jet flattens out into a sheet, or more precisely, a series or alternately orthogonal sheets. Figure 3.11 shows such a series with the first and third sheet visible edge-on and the second sheet in the imaging plane of the microscope. The visible sheet is 100 micrometres across and since it was produced from a circular jet 20 micrometres in diameter, a thickness of at most 2 micrometres is implied.

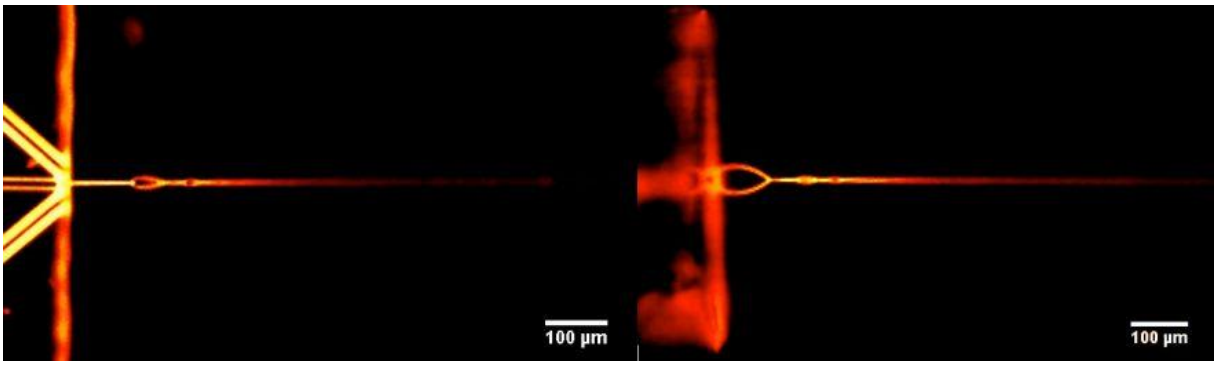

Figure 3.12: Optical micrographs viewed from in the plane of the device (left) and edge-on (right) rotated 90 degrees. This demonstrates the series of alternating orthogonal sheets generated as the fluid travels left to right in the figure.

At higher gas pressures the sheets become wider and thinner eventually breaking up close to the nozzle. Figure 3.12 shows two optical microscope images of the same nozzle rotated 90

This project has received funding from the *European Union's Horizon 2020 research and innovation programme* under grant agreement No 654220

degrees relative to each other. In the left image, the liquid channels are visible at the left of the image.

The thickness of the sheets has not been measured yet, but given that sheets as wide as 200 micrometres have been generated from a 20 micrometre cylindrical jet it is likely that the thickness is at most a few microns and more likely even thinner. Converging half angles of 20, 30, and 40 degrees were tested and sheets were produced with each microfluidic jet geometry. The 40 degree nozzles have so far performed best but due to the small sample size we have not yet determined the optimal geometry.

Further experiments with these devices will be done in future in order to optimise their use-ability for the purposes of liquid jet based timing tool development.

This project has received funding from the *European Union's Horizon 2020 research and innovation programme* under grant agreement No 654220

4 Synergy Aspects

There are obvious synergies stemming from having two different development projects for timing tool development at European XFEL and ELI Beamlines.

At the moment, there are two directions in the development of liquid-sheet based timing tool developments - macroscopic colliding-jet generated sheets and microfluidic sheets-jets based on the concept of the gas-dynamic virtual nozzle. The colliding-jet based sheets are beginning to see applications already, but recent efforts to create new types of low-consuming sample delivery systems for in-vacuum are a strong argument for the co-development of microfluidic-based timing tools for systems where deeper level of vacuum might be needed to achieve having smaller volume to be pumped into the chamber. Both approaches are promising - basic capabilities can be used for timing tool development, but both need to be further developed for the purpose.

The colliding-jet based approach is already an applicable development, for the microfluidic based system more research and development effort is needed (especially in the areas of identifying optimal methods for liquid micro-sheet generation, sheet characterization, and in designing timing method appropriate imaging optics and image acquisition); however the development already made for the macroscopic colliding jet system can be already then used to create a timing tool from the microfluidic system. Conversely, the experience from developing a reflection/spatial-encoding based tool for microfluidic system developed at kHz at ELI Beamlines could be utilized in the development of a comparable tool for MHz repetition rates at European XFEL. Due to the inherently better synchronization of the ultrashort X-ray and optical pulses at ELI Beamlines (both being generated just a few meters from each other from the originally single optical pulse), different approaches can be verified for later use at XFEL beamlines.

Last, but not least, developing general abilities for liquid sample delivery are important for both facilities. By sharing the efforts of learning about the control and characterization of both macroscopic and microfluidic sheets a significant benefit is created for the sample delivery development efforts of both the European XFEL and ELI facilities. In addition, sharing the work on development of a particular method, duplication of effort to resolve particular problems can be avoided. The methods developed and applied for the characterisation flat sheets will be applicable to the other types of jets, even round “Rayleigh jets” and the microfluidic GDVN jets.

This project has received funding from the *European Union’s Horizon 2020 research and innovation programme* under grant agreement No 654220

5 Conclusions

In this deliverable report, the capabilities of two different approaches for generation of liquid jet flat sheets are discussed with respect to their practical utilization as timing tools. The colliding-jets approach has proven to be able to generate flat sheets of acceptable parameters with respect to sheet geometry (1-2 mm width, down to 5 µm thickness) and liquid replacement speeds up to 50 m/s that are quite acceptable for applications at kHz repetition rates (including the laser driven X-ray and XUV sources of ELI Beamlines) and are close to acceptable speeds for the highest possible repetition rate of 4.5 MHz of the European XFEL.

The liquid sheet jet technique of liquid introduction can double as a sample introduction method, in some cases allowing for simultaneous running of an X-ray experiment and a timing tool analysis on the same liquid sample. For this purpose and for the purpose of timing soft X-ray/XUV pulses a more promising - but as of now less mature technique - is based on microfluidic gas-formed liquid micro-sheet. Preliminary experiments show that the microfluidic sheet technique allows for considerable reduction of liquid consumption - sheets approximately 100 µm in width and 1 µm in thickness were generated. The lower liquid volumetric flow (on the order of fractions of mL/h compared to up to several tens of mL/h in the colliding-jets approach) would aid in preserving of the vacuum environment required by soft X-ray/XUV light sources, as well as in maintaining sample economy when used as a sample delivery method.

Either sheet generation method will need to be complemented by an appropriate detection scheme. Currently developed spatial and spectral time encoding methods promise to achieve sub-10 fs uncertainty in the determination of the timing jitter (shot-to-shot). Achieving these parameters will be the main scope of work in the following period of the EUCALL project.

In future, it is also expected that the colliding-jet sheet technique will be implemented at the FXE scientific instrument and real data on X-ray timing will be gathered at reduced repetition rate, since full 4.5 MHz is expected only in 2018. The microfluidic sheet method which is being pursued by ELI Beamlines will be first tested with optical pump-probe setups due to the expected slower time in X-ray source deployment, while verification of the method at the European XFEL is still a possibility.

This project has received funding from the *European Union's Horizon 2020 research and innovation programme* under grant agreement No 654220

6 Summary

This report describes the efforts for developing a new type of tool that could be used to accurately measure the timing between X-ray and optical pulses of femtosecond length. The basis of this tool would be a flat liquid sheet that changes some of its properties when interacting with an X-ray pulse. Timing techniques that allow to measure the jitter between the arrival of X-ray and optical pulses already exist, but they have been used with non-replaceable solid samples. Since the solid targets would not survive in the direct beam at the expected high pulse energy and repetition rate of the upcoming X-ray beams of the European XFEL, the advantage of the liquid sheet concept compared to existing solid-based techniques is in the continuous renewal of the material of the sheet. At ELI Beamlines the microfluidic sheet development is strongly synergic to small-consumption sample delivery development that can support the timing tool development with its nearly jitter free X-ray/XUV generation schemes.

In this report, two arrival time detection schemes (spatial and spectral time encoding) and two options for creating such a flat sheet (colliding-jets and microfluidic sheet jet) are discussed. The considered detection methods employing either spatial or spectral time encoding when used on solid targets at low X-ray repetition rates have proven to be capable of compensating for timing jitter below 10 femtoseconds; similar performance is expected from the liquid-sheet based methods.

The liquid sheet method based on colliding-jets has been demonstrated to deliver dimensions and flow-rates needed for its implementation in a timing tool that would be capable of running at initial operational parameters of the X-ray beam of the European XFEL, similar liquid jet delivery system may be considered at ELI Beamlines for applications where large liquid volume or liquid consumption is not a constraint. Further optimizations of the liquid jet sheet may be needed to achieve readiness for the final high inter-train repetition rate of 4.5 MHz at the European XFEL. At ELI Beamlines, the pursued flat sheet option is based on a microfluidic gas-driven liquid jet system that has proven to be able to create thinner sheets and thus require smaller amount of liquid sample. However, since this option is less mature, more effort will be needed to develop an optimized design.

This project has received funding from the *European Union's Horizon 2020 research and innovation programme* under grant agreement No 654220

7 References

[Alt06] Altarelli, M. et al. *The European X-ray Free-Electron Laser Technical Design Report.* DESY-2006-097, ISBN 978-3-935702-17-1 (2006).

[Alt11] Altarelli, M. *The European X-ray free-electron laser facility in Hamburg*. Nucl. Instr. Meth. Phys. Res. B **269**(24), 2845–2849 (2011).

[BHW+14] Bionta, M. R., Hartmann, N., Weaver, M., French, D., Nicholson, D. J., Cryan, J. P., Glownia, J. M., Baker, K., Bostedt, C., Chollet, M., Ding, Y., Fritz, D. M., Fry, A. R., Kane, D. J., Krzywinski, J., Lemke, H. T., Messerschmidt, M., Schorb, S., Zhu, D., White, W. E., Coffee, R. N. *Spectral encoding method for measuring the relative arrival time between x-ray/optical pulses.* Rev. Sci. Instr. **85**, 083116 (2014).

[BAG+16] Britz, A., Assefa, T. A., Galler, A., Gawelda, W., Diez, M., Zalden, P., Khakhulin, D., Frenandes, B., Gessler, P., Sotuodi, H., Beckmann, A., Harder, M., Yavas, H., Bressler, C. *A multi-MHz single shot acquisition scheme with high dynamic range: pump-probe X-Ray experiments at synchrotrons*. J. Synchr. Rad. **23**, 1409-1423 (2016). DOI: 10.1107/S1600577516012625

[DBP+14] Danailov, M. B., Bencivenga, F., Capotondi, F., Casolari, F., Cinquegrana, P., Demidovich, A., Giangrisostomi, E., Kiskinova, M. P., Kurdi, G., Manfredda, M., et al. *Towards jitter-free pump-probe measurements at seeded free electron laser facilities.* Opt. Express **22** (11), 12869–12879 (2014). DOI: 10.1364/OE.22.012869.

[DL13] Decking, W., Limberg, T. *European XFEL Post-TDR Description*. XFEL.EU TN-2013-004-01 (2013).

[Dur12] Durbin, S. *X-Ray Induced Optical Reflectivity*. AIP Advances **2**(4): 1–8 (2012). doi:10.1063/1.4768803.

[DWS+08] DePonte, D. P., Weierstall, U., Schmidt, K., Warner, J., Starodub, D., Spence, J. C. H., Doak, R. B. *Gas Dynamic Virtual Nozzle for Generation of Microscopic Droplet Streams*. J. Phys. D. Appl. Phys. **41**, 195505 (2008). DOI:10.1088/0022-3727/41/19/195505.

[EBP+15] Eckert, S., Beye, M., Pietzsch, A., Quevedo, W., Hantschmann, M., Ochmann, M., Ross, M., Minitti, M. P., Turner, J. J., Moeller, S. P., Schlotter, W. F., Dakovski, G. L., Khalil, M., Huse, N., Fölisch, *A. Principles of femtosecond X-ray/optical cross-correlation with X-ray induced transient optical reflectivity in solids.* Appl. Phys. Lett. **106**, 061104 (2015).

[ELIWEB] Website of the ELI Beamlines project, URL: http://www.eli-beams.eu/

[EQF+15] Ekimova, M., Quevedo, W., Faubel, M., Wernet, P., Nibbering, E. T. J. *A liquid flatjet system for solution phase soft-x-ray spectroscopy*. Structural Dynamics **2**, 054301 (2015).

[GAB+08] Gahl, C., Azima, A., Beye, M., Deppe, M., Döbrich, K., Hasslinger, U., Hennies, F., Melnikov, A., Nagasono, M., Pietzsch, A., Wolf, M., Wurth, W., Föhlisch, A. *A*

This project has received funding from the *European Union's Horizon 2020 research and innovation programme* under grant agreement No 654220

Femtosecond X-Ray/optical Cross-Correlator. Nature Photonics **2** (3): 165–169 (2008). DOI:10.1038/nphoton.2007.298.

[HCB+13] Harmand, M., Coffee, R., Bionta, M. R., Chollet, M., French, D., Zhu, D., Fritz, D. M., Lemke, H. T., Medvedev, N., Ziaja, B., Toleikis, S., Cammarata, M. *Achieving few-femtosecond time-sorting at hard X-ray free-electron lasers.* Nat. Phot. **7**, 215-218 (2013).

[HGR+10] Hallmann, J., Grübel, S., Rajkovic, I., Quevedo, W., Busse, G., Scholz, M., More, R., Petri, M., Techert, S. *First Steps towards Probing Chemical Systems and Dynamics with Free-Electron Laser Radiation – case studies at the FLASH Facility.* J. Phys. B: At. Mol. Opt. Phys. **43** (19): 194009 (2010). DOI:10.1088/0953-4075/43/19/194009.

[KOT+16] Katayama, T., Owada, S., Togashi, T., Ogawa, K., Karvinen, P., Vartiainen, I., Eronen, A., David, C., Sato, T., Nakajima, K., Joti, Y., Yumoto, H., Ohashi, H., Yabashi, M. *A Beam Branching Method for Timing and Spectral Characterization of Hard X-Ray Free-Electron Lasers*. Structural Dynamics **3** (3), 1–15 (2016). DOI:10.1063/1.4939655.

[KTS+12] Krupin, O., Trigo, M., Schlotter, W. F., Beye, M., Sorgenfrei, F., Turner, J. J., Reis, A. A., Gerken, N., Lee, S., Lee, W. S., Hays, G., Acremann, Y., Abbey, B., Coffee, R., Messerschmidt, M., Hau-Riege, S. P., Lapertot, G., Lüning, J., Heimann, P., Soufli, R., Fernandez-Perea, M., Rowen, M., Holmes, M., Molodtsov, S. L., Föhlisch, A., Wurth, W. *Temporal Cross-Correlation of X-Ray Free Electron and Optical Lasers Using Soft X-Ray Pulse Induced Transient Reflectivity.* Optics Express **20** (10), 11396 (2012). DOI:10.1364/OE.20.011396.

[MCW+08] Maltezopoulos, T., Cunovic, S., Wieland, M., Beye, M., Azima, A., Redlin, H., Krikunova, M., Kalms, R., Frühling, U., Budzyn, F., Wurth, W., Föhlisch, A., Drescher, M. *Single-Shot Timing Measurement of Extreme-Ultraviolet Free-Electron Laser Pulses*. New Journal of Physics **10**, 033026 (2008). DOI:10.1088/1367-2630/10/3/033026.

[OKS+11] Omar, E., Karim, A., Schmidhammer, U., Jeunesse, P., Larbre, J.-P., Lin M., Muroya, Y., Katsumura, Y., Pernot, P., Mostafavi, M. *Time-Dependent Radiolytic Yield of OH• Radical Studied by Picosecond Pulse Radiolysis.* The Journal of Physical Chemistry. A **115** (44): 12212–16 (2011). DOI:10.1021/jp208075v.

[SGB+15] Schulz, S., Grguras, I., Beherens, C., Bromberger, H., Costello, J. T., Czwalinna, M. K., Felber, M., Hoffmann, M. C., Ilchen, M., Liu, H.Y., Mazza, T., Meyer, M., Pfeiffer, S., Predki, P., Schefer, S., Schmidt, C., Wegner, U., Schlarb., H., Cavalieri, A. L. *Femtosecond all-optical synchronization of an X-ray free-electron laser*. Nat. Commun. **6**:5938 (2015).

[SML+16] Stan, C. A., Milathianaki, D., Laksmono, H., Sierra, R. G., McQueen, T. A., Messerschmidt, M., Williams, G. J., Koglin, J. E., Lane, T. J., Hayes, M. J., Guillet, S. A. H., Liang, M., Aquila, A. L., Willmott, P. R., Robinson, J. S., Gumerlock, K. L., Botha, S., Nass, K., Schlichting, I., Shoeman, R. L., Stone, H. A., Boutet, S. *Liquid explosions induced by X-ray laser pulses*. Nat. Phys. **12**, 966-972 (2016).

This project has received funding from the *European Union's Horizon 2020 research and innovation programme* under grant agreement No 654220

[STO+15] Sato, T., Togashi, T., Ogawa, K., Katayama, T., Inubushi, Y., Tono, K., Yabashi, M. *Highly Efficient Arrival Timing Diagnostics for Femtosecond X-Ray and Optical Laser Pulses*. Applied Physics Express **8** (1), 012702 (2015). DOI:10.7567/APEX.8.012702.

[BKL+95] Braun A., Korn G., Liu X., Du D., Squier J., and Mourou G., *Self-channeling of high-peak-power femtosecond laser pulses in air*, Optics Letters **20**, 73-75 (1995). DOI: 10.1364/OL.20.000073

[TKD+14] Trebbin, M., Krüger, K., DePonte, D., Roth, S. V., Chapman, H. N., Förster, S. *Microfluidic liquid jet system with compatibility for atmospheric and high-vacuum conditions*. Lab Chip **14**, 1733–1745 (2014). DOI:10.1039/c3lc51363g.

[YKK+11] Yang, J., Kondoh, T., Kan, K., Yoshida, Y. *Ultrafast Pulse Radiolysis*. Nuclear Instruments and Methods in Physics Research Section A: Accelerators, Spectrometers, Detectors and Associated Equipment **629** (1), 6–10 (2011). DOI:10.1016/j.nima.2010.11.109.

This project has received funding from the *European Union's Horizon 2020 research and innovation programme* under grant agreement No 654220

8 Publications

So far, there have been no peer-reviewed publications on the subject discussed in this report.

Beside the report on the progress at the Annual Meeting of the EUCALL project, and various PUCCA meetings the EUCALL project in general and status of the timing tool developments in particular had been disseminated on a poster at the Annual Meeting of the Hamburg Centre for Ultrafast Imaging (CUI) in Hohwacht, Germany, in October 2016. The CUI is one of the clusters of excellence of the University of Hamburg.

This project has received funding from the *European Union's Horizon 2020 research and innovation programme* under grant agreement No 654220

9 Acknowledgments

We acknowledge the support and contributions of R. Graceffa, P. Vagovič and T. Sato (European XFEL GmbH, Hamburg, Germany) as well as D. P. DePonte, J. D. Koralek, and P. O. Mgbam from the Linac Coherent Light Source (LCLS), SLAC National Accelerator Laboratory, California, USA.

S. Schulz acknowledges additional funding from the Hamburg Centre for Ultrafast Imaging (CUI). The CUI is one of the clusters of excellence of the University of Hamburg.